University of Stuttgart

DLR Design Challenge
SoSe 2024

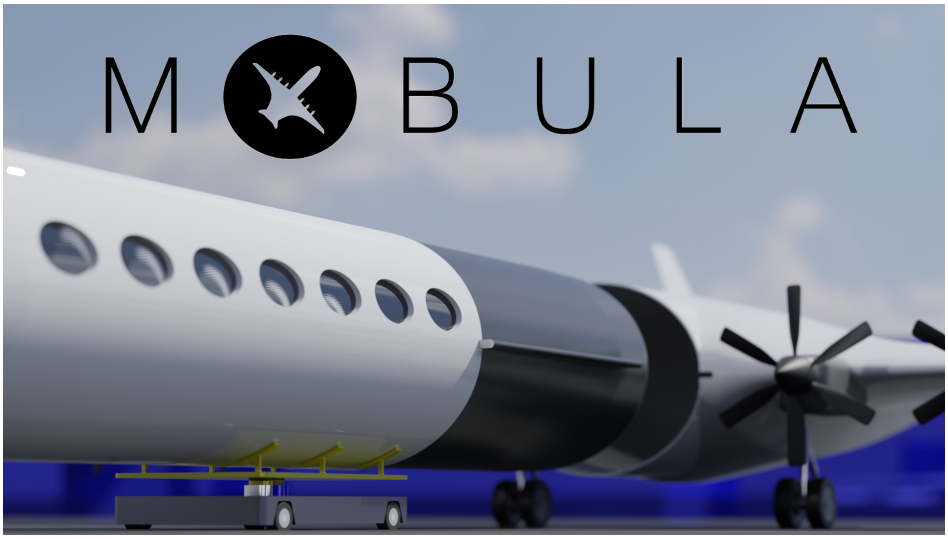

Modular Blended Wing Body Ultra Low Emission Aircraft

Bernhardt, Arthur (3409404)

Fuchs, Felix (3382916)

Haas, Fabian (3634965)

Wolf, Felix (3389841)

Wolf, Luka (3392702)

Wössner, Lars (3383453)

Submitted:
21.07.2024
Supervisor:
M.Sc. JOHANNES SCHNEIDER

Team Members

Arthur Bernhardt
4th semester M. Sc.
Simulation

Felix Fuchs
5th semester M. Sc.
Propulsion & Operations

Fabian Haas
5th semester M. Sc.
Structure

Felix Wolf
3rd semester M. Sc.
Propulsion & Operations

Luka Wolf
3rd semester M. Sc.
Aerodynamics

Lars Wössner
3rd semester M. Sc.
Structure

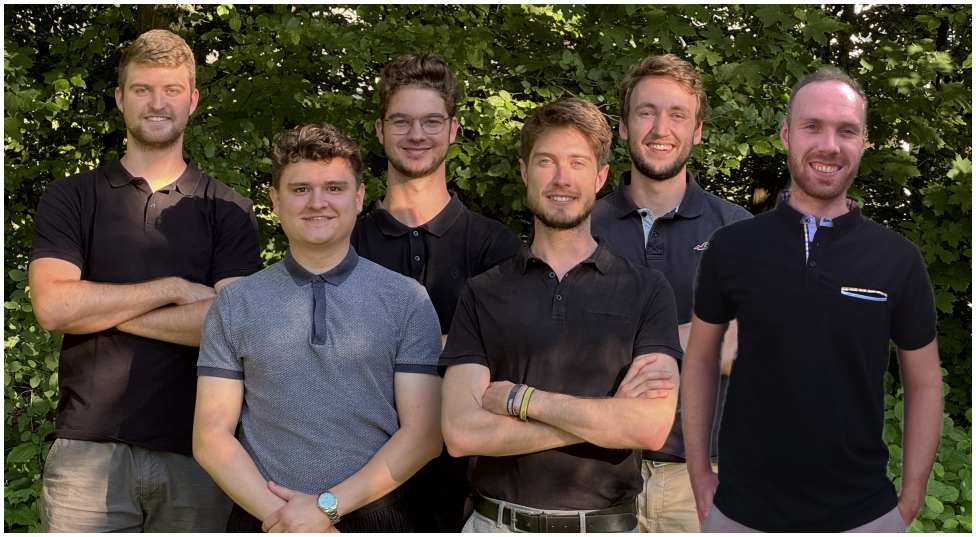

Abstract

This technical report presents the revolutionary design of a regional aircraft. It is the subject of participation in the DLR Design Challenge 2024. The project called MOBULA (MOdular Blended wing body Ultra Low emission Aircraft) is our innovative solution to the task given by the DLR Jury. It meets the requirements of an environmentally friendly and energy-efficient aircraft operating at attractive costs. The entry into service year is set to 2050. First, the given route network and passenger demand is analyzed to determine the seat number of 72 passengers. The hybrid blended wing body configuration is selected by an evaluation matrix. Its standout feature is the modular design, allowing the cabin and wing body to separate on the ground for boarding. This design includes an innovative wing configuration and an advanced propulsion system, utilizing a battery-fuel cell hybrid. Initially, the model is created in a CAD program, and its aerodynamic characteristics are simulated using basic CFD tools. The dimensions of the propulsion system and component masses are calculated with the support of MATLAB tools. Results indicate that the modular concept can reduce the turnaround time by 40% compared to conventional regional turboprops. In flight, the energy consumption is reduced to 5.5 kWh per 100 available seat kilometers (ASK). MOBULA features a range of 1500 km, plus additional diversion range of 250 km. In conclusion, the presented design demonstrates that modular aircraft concepts, such as MOBULA, can achieve higher efficient operations for regional air transportation. The substantial reduction of operating costs and energy consumption are outlined in this report. The concept offers high flexibility to react to future applications and changing market demands.

Zusammenfassung

Dieser technische Bericht stellt das revolutionäre Design eines Regionalflugzeugs vor. Es ist Gegenstand der Teilnahme an der DLR Design Challenge 2024. Das Projekt mit dem Namen MOBULA (MOdular Blended wing body Ultra Low emission Aircraft) ist unsere innovative Lösung für die von der DLR-Jury gestellte Aufgabe. Es erfüllt die Anforderungen an ein umweltfreundliches und energieeffizientes Flugzeug, das zu attraktiven Kosten operiert. Das Entry into service Jahr ist auf 2050 festgelegt. Zunächst wird das gegebene Streckennetz und die Passagiernachfrage analysiert, um die Sitzplatzzahl von 72 Passagieren zu bestimmen. Aus einer Bewertungsmatrix wird die Hybrid Blended Wing Konfiguration ausgewählt. Das charakteristische Merkmal von MOBULA ist das modulare Konzept. Der Kabinenteil und der Flügelteil werden am Flughafen geteilt. Das Design zeichnet sich durch eine innovative Flügelkonfiguration und ein fortschrittliches Antriebssystem aus, das aus einem Batterie-Brennstoffzellen-Hybrid besteht. Das Modell wird zunächst in einem CAD-Programm erstellt und seine aerodynamischen Eigenschaften werden mit einfachen CFD-Tools simuliert. Das Antriebssystem und die Struktur-Komponenten werden mit MATLAB-Tools ausgelegt. Die Ergebnisse zeigen, dass durch das modulare Konzept die Turnaround-Zeit im Vergleich zu konventionellen Regionalflugzeugen um 40% reduziert werden kann. Im Flug wird der Energieverbrauch auf 5,5 kWh pro 100 ASK reduziert. MOBULA hat eine Reichweite von 1500 km, zuzüglich einer Diversion von 250 km. Zusammenfassend zeigt das vorgestellte Design, dass modulare Flugzeugkonzepte wie MOBULA einen effizienteren Betrieb im regionalen Luftverkehr ermöglichen können. Die erhebliche Senkung der Betriebskosten und des Energieverbrauchs wird in diesem Bericht dargelegt. Das Konzept bietet eine hohe Flexibilität, um auf zukünftige Anwendungen und sich ändernde Marktanforderungen zu reagieren.

Contents

List of Figures

List of Tables

List of Symbols

α_i	Angle of incidence	[°]
b	Wingspan	[m]
C_D	Drag coefficient	[-]
C_L	Lift coefficient	[-]
D	Drag	[N]
E	Glide ratio	[-]
F	Thrust power	[N]
F_{max}	Maximum force	[N]
$F_{ultimate}$	Ultimate load	[N]
g	Gravitational acceleration	[m/s²]
γ	Climb angle	[°]
h	Cruise altitude	[m]
η_{grav}	Gravimetric storage density	[Wh/kg]
η_p	Propeller efficiency	[-]
L	Lift	[N]
L/D	Lift over drag	[-]
l_μ	MAC	[m]
Λ	Aspect ratio	[m]
Ma	Mach number	[-]
m_c	Contingency mass	[-]
m_E	End mass	[kg]
m_f	Fuel mass ratio	[-]
m_{mtom}	Maximum takeoff mass	[kg]
m_{mzfm}	Maximum zero fuel mass	[kg]
m_S	Start mass	[kg]
m_{tank}	Tank mass	[kg]
P	Power	[W]
P_{max}	Maximum power	[W]
Re	Reynolds number	[-]
ROC	Climb rate	[m/s]
ROD	Descent rate	[m/s]
R	Range	[km]
S	Wing surface	[m²]
SFC	Specific fuel Consumption	[N/J]
S_{ref}	Reference area	[m²]
u	Blade wingtip velocity	[m/s]
v	Cruise speed	[m/s]
$v_{landing}$	Approach speed	[m/s]

List of Abbreviations

AOA	Angle Of Attack
ASK	Available Seat Kilometer
DOC	Direct Operating Costs
FC	Fuel Cell
GSE	Ground Support Equipment
HBWB	Hybrid Blended Wing Body
MAC	Mean Aerodynamic Chord
MOBULA	Modular Blended Wing Body Ultra Low Emission Aircraft
MTOM	Maximum Takeoff Mass
MZFM	Maximum Zero Fuel Mass
OME	Operation Mass Empty
PAX	Passengers
PEM	Proton Exchange Membrane
PEMFC	Proton Exchange Membrane Fuel Cell
SFC	Specific Fuel Consumption
SSB	Solid State Battery
TRL	Technology Readiness Level

1 Introduction

The development of an environmentally friendly short-haul aircraft is important due to the ongoing climate change and the transformation of the energy and mobility sector. As the demand for air travel increases it is crucial to address the environmental impact of aviation. Short-haul flights significantly contribute to carbon emissions. Therefore, it is essential to develop an aircraft that is eco-friendly and cost-efficient to reduce the environmental footprint of aviation. The motivation of the DLR Challenge is to identify sustainable and innovative concepts that can maintain the efficient transport of people and ensure economic viability. The challenge task involves designing an aircraft that meets the efficiency and cost-effectiveness requirements of a specific network of European regional routes.
The MOBULA team has therefore set itself the goal of designing an aircraft that meets these criteria. MOBULA stands for **MO**dular **B**lended wing body **U**ltra **L**ow emission **A**ircraft to sum up the key features of the concept. The aircraft aims to reduce carbon emissions by using an advanced propulsion system and optimizing energy efficiency. The focus is on reducing turnaround time and minimizing noise emissions. Hence, the route network is characterized by short routes at high frequency, thus high numbers of flight cycles.
Reducing turnaround time is attractive for both passengers and airlines, as it leads to shorter stays at the airport and cost reduction. Noise reduction is beneficial for airport surroundings. It also contributes to lower landing fees and leads to a quieter and more pleasant flight for the passengers. MOBULA is planning a modular design for the aircraft to allow for future upgrades and modifications. This ensures that the aircraft can be adapted to new technologies and environmental standards throughout its operational life. This concept rethinks the way of regional air travel for more efficient operations at a greener footprint.
In this technical report, first the design process is described in chapter 2. Followed by that all the details of the aircraft concept such as aerodynamics, propulsion and structure are outlined in chapter 3. Finally, the operations that include the airport and boarding concepts, cabin layout, and direct operating costs are discussed in the concluding chapter 4.

2 Design Process

The design process was guided by the iterative process used in the industry for aircraft design. First, the market demand is analysed. In preliminary design the configuration and the essential sizing parameters are fixed for the following concept development.

2.1 Market & Network Analysis

The route Network and data of the passenger demand was given by the jury. A crucial part of our task is to determine the optimal passenger capacity for our aircraft design. To achieve this, we analyzed capacity utilization for seat configurations ranging from 60 to 120 passengers (PAX). The available slots at Hamburg Airport are limited, with a specified range of 142 to 276 slots, posing a constraint for this task. As a result of the simulations there were four options to choose from: 60, 72, 92 and 119 PAX. The choice was made for the 72-passenger configuration, as it allows comparison with the ATR 72-200. The selection of seat number is shown in Figure 2.1.

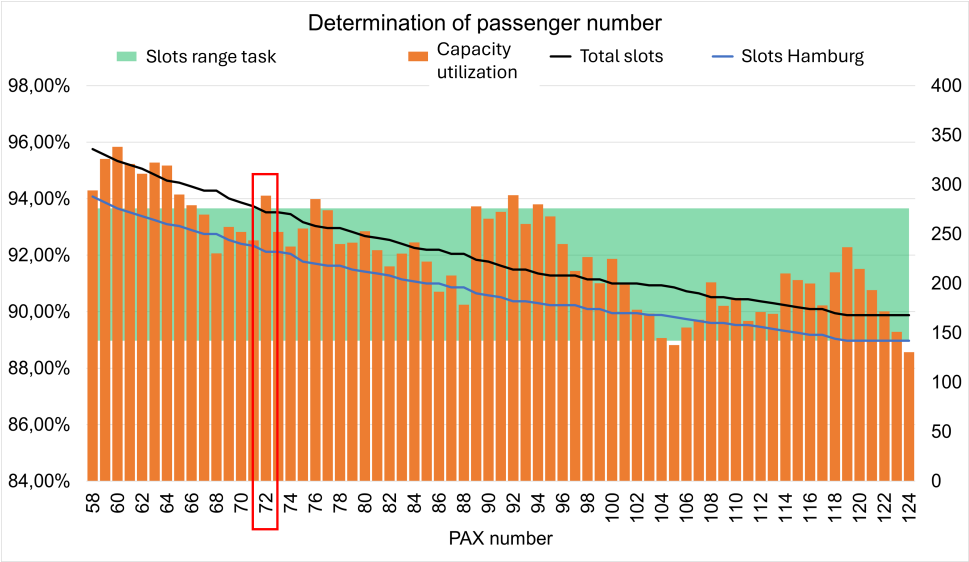

Figure 2.1: Selection of passenger number regarding slot restrictions in HAM

The chosen number allows to design a cabin layout with 12 rows by six seats abreast. It is also one of the middle options, so there is more freedom for optional design changes in seat numbers at a later stage, still complying with the task requirements. As a consequence, the utilization of slots in Hamburg is 232 and is 272 slots including all airports. To fulfill the route network requirements the routes without stopovers on longer flight (e.g. BRI to HAM) are considered. This determines the required range for the aircraft and thus the design of the propulsion system.

2.2 Preliminary Design

After the market analysis different aircraft configurations are considered for the Preliminary Design. In order to establish evaluation criteria, the top level requirements (TLR) for our case have to be discussed. There are already requirements set from the assignment, e.g. the climb and descent angle or the take-off distance. However, there is also space for TLR that we set for our own design.

The conclusion of our internal discussion are described in the following three major TLR, which serve as orientation for the following design of the airplane:

1. Reduction of turnaround time
2. Low-noise emissions
3. Distributed propulsion

At that early stage of the process a wide range of typical, but also unconventional aircraft configurations were examined such as (Hybrid) Blended Wing Body, three-surface or boxwing. After scientific research and first calculations using e.g. Torenbeek the main configurations were evaluated. For that, more aerodynamic and qualitative parameters were added to our TLR. They were quantified and accumulated into a total score for each configuration. Each of them referred to the ATR 72-200 version as a basic model. The results are summarized in an evaluation matrix that is the basis for the selection.
As a consequence, there were two configurations to choose from: The Hybrid and the Blended Wing Body. Both have significant aerodynamic advantages over the other designs for an energy-efficient cruise. Though the Hybrid Blended Wing Body (HBWB) is beneficial over the Full Blended Wing regarding passenger comfort and accessibility. For that reason, we chose the HBWB as the basis for further development in the aircraft's design. It combines the large surface area and so a high-lift configuration of the Blended Wing and the operability of conventional tube and wing.
More important the HBWB offers the best configuration for the hybrid propulsion architecture, which is described in more detail in chapter 3.4, especially for using hydrogen. Using this fuel is quite challenging for conventional aircraft designs. In tube and wing configuration the hydrogen has to go a long way from the tanks in the back to the engines on the wing. With the unconventional configuration of MOBULA the distances from the hydrogen tanks to the fuel cells in the pods below the wing are shorter. Another benefit is that the lines do not have to cross the cabin or fuselage. Therefore, first, more safety for passengers is guaranteed and second, the energy consumed for heating the fuel from cryogenic to operating temperatures is reduced.
At the same point, we rethought the organisation of the turnaround and boarding at airports. With the intention to reduce the turnaround time significantly, the idea is to build the plane in a modular way. The key difference is to split it into cabin and flying wing body on ground and link the two parts for flight. The operations of the aircraft are explained in more detail in chapter 4.

Design Point

The calculations for the restrictive curves in the sizing diagram incorporate requirements for take-off distance, climb, and descent angle respectively. The sizing requirement parameters, as shown in Table 2.1, are established as part of this task.
The resulting airplane design diagram (Figure 2.2) highlights a strategically selected design point, positioned as low as possible to optimize the power-to-weight ratio. From this design point, we determined the necessary wing area and power requirements for the aircraft. As a hybrid blended wing, the aircraft features significantly more wing area than a conventional design, resulting in a lower wing load. We chose a design point with a lower power-to-weight ratio and reduced wing load over one with a higher power-to-weight ratio and increased wing load to enhance fuel efficiency. In this point the wing loading is 188.6 kg/m² and the power loading is 18.5 W/N. This decision aligns with the primary goal of the design challenge: creating an energy-efficient aircraft.

Table 2.1: Sizing requirement parameters

Sizing Requirements		
No.	Parameter	Value
1	Takeoff distance	<1510 m
2	Climb angle	>4°
3	Descent angle	>5.5°
4	Average passenger mass	95 kg
5	Entry into service	2050
6	Diversion Range	250 km

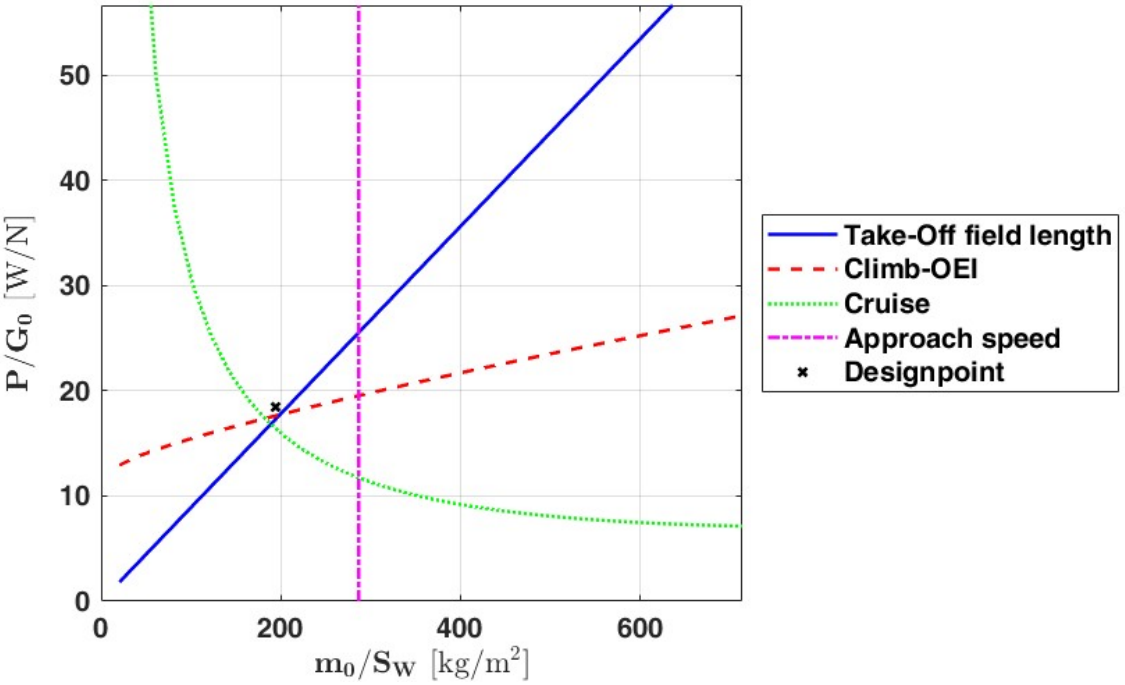

Figure 2.2: Design Diagram

Upon determining the design point, the preliminary design is considered complete. The next steps involve detailed sizing and further development of the MOBULA design.

3 Aircraft Concept

MOBULA has a characteristic design which stands out from other regional airplanes. This overview presents the aircraft's concept and shows the relevant information of its components. Further the results of detailed calculations and simulations are displayed.

3.1 Overview & Key Technologies

An overview of the aircraft dimensions is given in Figure 3.1.

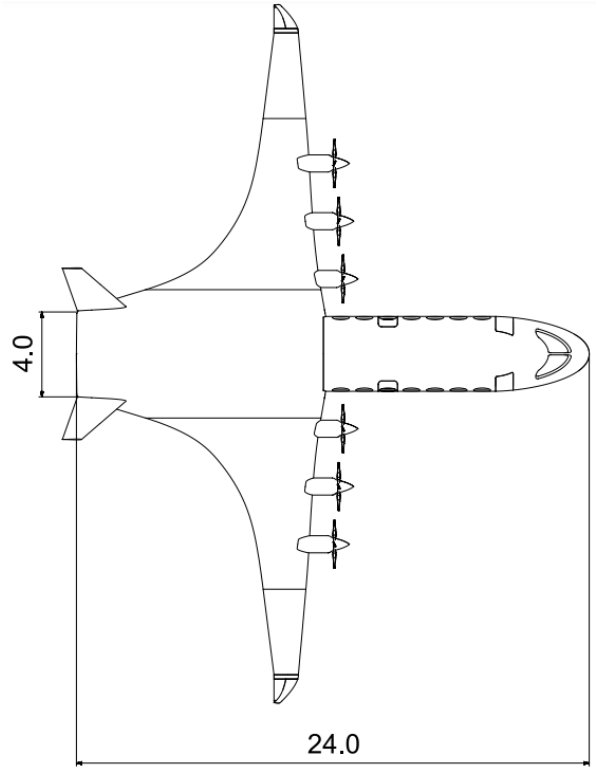

(a) Top perspective

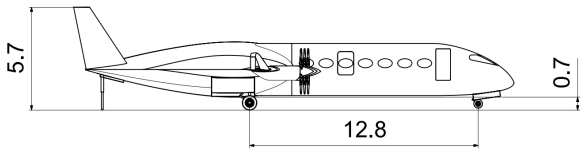

(b) Side perspective

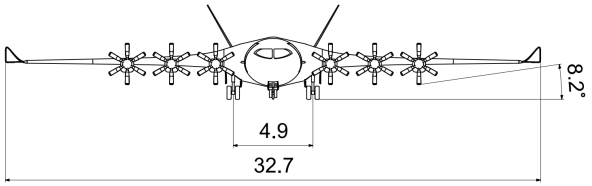

(c) Front perspective

Figure 3.1: Three-side view

The key feature of MOBULA is the modularity and its ability to be split into two independent bodies. There was research already to build airplanes with a pod to attach. However, this particular concept is new. The way of coupling the two parts together was not investigated deeply in research before, although it uses long-used mechanisms which are already in-service for instance for trains. The link is further explained in the associated chapter 3.5. It is assumed that it has already reached high technology readiness but has to be tested in flight-similar environment, although it should not essentially affect the coupling behaviour and safety because the detachment and docking is exclusively operated on the ground.
The detachment and docking process is further expanded on in chapter 4.1.

Table 3.1: Technology Readiness Level of key technologies

Technology Readiness Level (TRL)		
Technology	TRL (2024)	TRL estimation (2050)
Coupling	8	9
Solid State Battery (Li-metal)	3	8
Modular Hydrogen Tanks	6	9
PEM Fuel Cell	5	8-9

For future TRL predictions there are only estimations to be made on scientific base. The entry into service (EIS) date is set to 2050 in the task. The TRL estimations for all key technologies of MOBULA are listed in Table 3.1 and their positioning in the aircraft is shown in Fig. 3.2. The solid state battery (SSB) is currently still under experimental research [14]. As it is a promising battery technology SSB are about to reach TRL 7 already in 2030 [20]. The integration of SSB in automotive applications in this decade supports that estimation.
There is also much research going into interchangeable hydrogen tanks formed in different shapes. The design decision was made towards cylindrical tanks because they are considered to be the most promising variant to store liquid hydrogen for the EIS. The amount of knowledge from storing gaseous hydrogen in cylindrical tanks can be used. They are also easy to handle in comparison to other shapes. A good example to show the modular exchanging hydrogen tanks during the turnaround is the company Universal Hydrogen. They already retrofit existing regional aircraft with hydrogen propulsion and they support the build-up of the hydrogen system around airplanes.

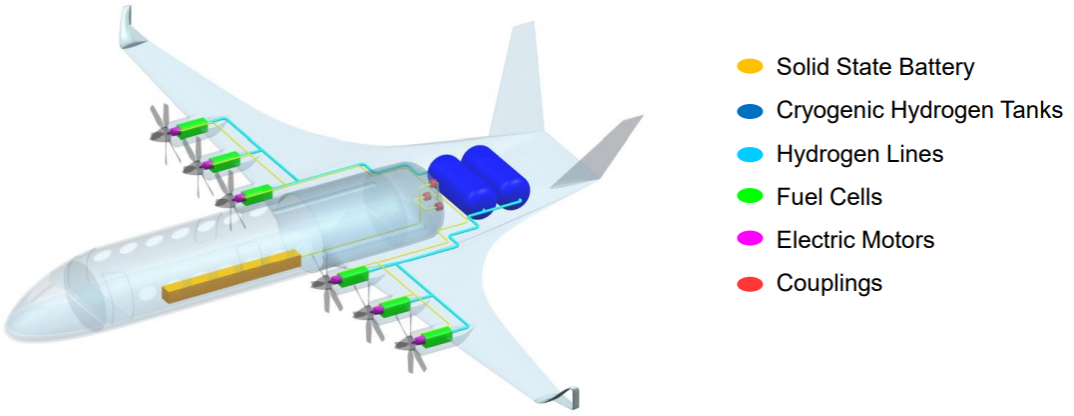

Figure 3.2: Assembly of key features

Using Fuel Cells to propel aircraft is not a new idea. The challenge of today is to bring them to power levels in the 1 to 2 MW area. Many research institutes, e.g. DLR, are working on performance and simulating proton exchange membrane fuel cells (PEMFC) and its system. The "DLR Exact" program and the projects of its institutes is one of them to name. According to [16] PEMFC are available for regional planes by 2035–2045 and therefore earlier than e.g. solid oxide fuel cells.

3.2 Configuration

The modular concept of MOBULA requires a special configuration. To integrate the hybrid propulsion system a blended wing design was chosen. That comes with specific arrangements for the primary and secondary structure.

Wing Geometry

The HBWB aircraft combines the advantages of a traditional fuselage with the aerodynamic efficiency of a blended wing design. This section provides an analysis of the wing geometry, focusing on the wing shape and the tail configuration. The wing of the HBWB is designed with a smooth transition from the fuselage to the wing enhancing aerodynamic efficiency by reducing interference drag. The wing has a high aspect ratio which is beneficial for reducing induced drag and improving the lift-to-drag ratio during cruise flight. The wing's trailing edge is designed with control surfaces such as flaps and ailerons, essential for controlling the aircraft during various phases of flight.

The resulting reference surface area has to be determined because it is not as great as the total surface area of the wing body. By examining the lift distribution of the wing area, it becomes clear that the outer wing sections contribute significantly more lift than the center body. This is due to the fact that the center body of the HBWB does not produce any substantial lift because of its symmetric airfoil profile, which is designed primarily for structural and balance purposes rather than for generating lift.
To ensure the accuracy of our aerodynamic analysis we exclude the center body from our calculations. As a consequence the reference surface area of the aircraft is determined to be 114 m². This adjustment reflects a more realistic outcome and aligns better with the actual aerodynamic performance of the aircraft. All major geometric parameters of the wing are summarized in Table 3.2.

Table 3.2: Wing dimensions

Wing parameters		
Wingspan	b	32.7 m
MAC	l_μ	5.4 m
Wing surface	S	164 m²
Reference area	S_{ref}	114 m²
Aspect ratio	Λ	10.1
Taper ratio	λ	0.1717

Control Surface Areas

Consideration of various tail designs led to the decision to install a V-shaped tail at the rear of the HBWB, which is an uncommon feature compared to traditional airplanes. This V-tail design integrates the functions horizontal and vertical stabilizers. This configuration offers several advantages, including reduced drag by combining the control surfaces. Therefore reducing the total wetted area and skin friction drag which improves overall aerodynamic efficiency and fuel efficiency.
The negative effect of higher trim drag is outweighed by the fact that the variation of the center of gravity over the total flight distance is very low. This stability is due to the use of hydrogen and batteries instead of conventional kerosene in the wing tanks, where the fluctuations in the center of gravity are greater. The innovative design represents a significant advance in aircraft

design as it combines the best features of conventional and blended wing body configurations. The airflow around the tailplane and the resulting vorticity is shown in Figure 3.3.

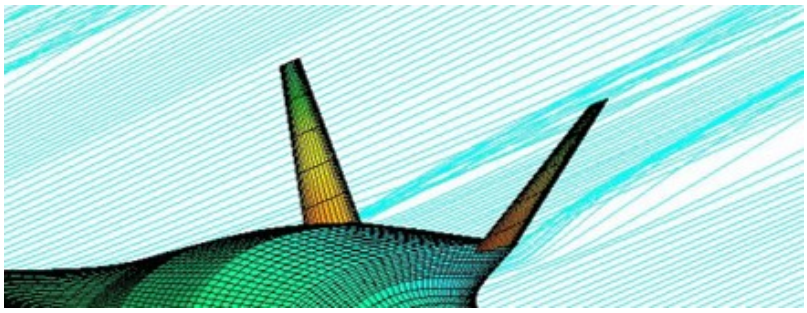

Figure 3.3: V-Tail Empennage

Similar assumptions as to the wing design must be made to calculate the dimensions of the tail. Conventional approaches like Raymer and others cannot be applied to V-tails of blended wing bodies. First, the actual reference surface area (114 m^2) has to be taken into account. Further, having a look on MOBULA's design, it is obvious that only the front half of the wing body actually has a lever arm to the tailplane. Therefore, the reference surface for dimensioning the control plane is approximately two-thirds of the total wing area. Regarding the assumptions, the total surface area of the empennage results in 25 m^2. Simulations were made using OpenVSP and FlightStream to investigate and validate the rear surface. These tools enabled an analysis of the aerodynamic properties and performance. An important criteria for its design is also the integrability in the general concept of MOBULA. There is ongoing research to find new methods to improve accuracy of those results. That scientific work is yet under investigation and thus not available in our aircraft design process.
For more horizontal stability, there is a pitch control installed in between the V-tailplane. The rudder at the rear edge of the center body supports the main empennage at critical pitch angels, e.g. at takeoff, landing and maneuvers. It also balances out the pitch-down moments that result from the lift of the large wing area.

Winglets

It is a crucial task to reduce the drag of the aircraft. Among many ways to reduce the lift-induced drag, winglets are one of them. Over the past decades numerous configurations of winglets have been developed, each with different advantages and disadvantages. After consideration we selected the spiroid winglet, as shown in Figure 3.4, due to its innovative design and promising performance improvements. Comparative studies indicate that the spiroid winglet offers several benefits over both a clean wing and traditional winglet designs.

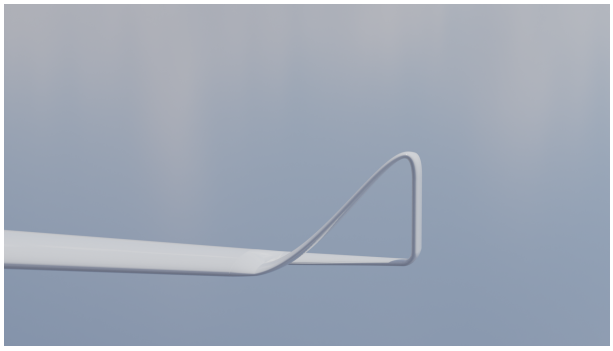

Figure 3.4: Spiroid

The spiroid winglet shows an reduction in lift-induced drag and additionally increases the overall lift of the aircraft. This leads to an improvement in the lift-to-drag ratio. Additionally, the spiroid winglet also contributes to delaying wing stall and provided better post-stall behaviour [11]. Despite the promising results, due to the fact that they are based on preliminary studies, further research is necessary to validate them. Therefore, our calculations did not take those factors into account.

3.3 Aerodynamics

The aerodynamics section addresses all relevant design decisions related to the wings, the empennage, and the entire aircraft. Programs such as XFLR5, OpenVSP and FlightStream were used to determine the profiles and wing masses and record aerodynamic values.

Wing Planform Selection

The general mission design is crucial for the wing planform design. The focus of the aerodynamic concept of the plane is on the drag coefficient. Due to our goal to obtain a low fuel consumption, decreased CO2 Emissions and minimized noise, the wing planform must be optimized to ensure aerodynamic efficiency. This involves careful consideration of factors such as aspect ratio, taper ratio, wing sweep and airfoil shape, all of which contribute to reducing induced and parasitic drag. As a result, iterative computational simulations are employed to refine the wing planform, balancing the trade-offs between aerodynamic performance, structural demands, and environmental impact.

Airfoil Selection

The airfoils are chosen based on the primary flight phase to achieve maximum aerodynamic efficiency. Therefore the airfoils are designed for the dominating phase, the cruise. While also fulfilling the restrictions by the remaining flight phases. The HBWB is divided into two parts: the center body and the outer wing. Due to the increased surface area of the aircraft, a symmetrical NACA 4-digit airfoil profile is selected for the center body. The symmetrical airfoil design is also chosen to simplify the connection between the fuselage and the wing. It is also recognized that a high lift coefficient with a high camber results in a relatively more negative moment coefficient which can negatively impact on longitudinal stability. The choice of a symmetrical airfoil is made because they offer consistent aerodynamic performance across a range of angles of attack (AOA), providing predictable and stable behavior [3], [7]. Additionally, symmetrical profiles are structurally robust and easier to manufacture to ensure durability and reliability. The outer wing is intended to contribute more to lift production. Various airfoil profiles are compared to determine their aerodynamic performance characteristics. Laminar, high lift and supercritical profiles are evaluated. The goal is to identify the profile that offers a low drag coefficient and a good lift-to-drag ratio and efficiency across a range of operating conditions.The calculation of the airfoils is performed in XFLR5. A laminar profile is selected for its superior performance characteristics for our needs.

The NACA 65(2)-415 laminar airfoil is chosen for the outer wing of the aircraft due to its significant advantages in reducing drag and improving fuel efficiency during cruise flight. Laminar airfoils are characterized by a smooth surface structure and a specific shape that maintains laminar flow over a larger portion of the wing [26]. The aircraft is designed to utilize a laminar airfoil and features a low wing sweep. This design is crucial for preserving the laminar flow and minimizing turbulence. By minimizing wing sweep the laminar region on the wing is maximized and fully leveraging the benefits of the laminar airfoil. Operating in the subsonic speed

range of Mach 0.4 to 0.5 the NACA 65(2)-415 laminar airfoil offers optimal performance characteristics [13], [23]. The laminar flow significantly contributes to higher efficiency by reducing energy losses due to friction. This results in lower fuel consumption and increased aircraft range. These advantages make the NACA 65(2)-415 airfoil particularly suitable for use on the outer wing. The transition between the symmetrical NACA 4-digit profile of the center body and the laminar profile occurs over a short distance. This smooth transition ensures aerodynamic efficiency and structural integrity.

Aerodynamic Validation

The following aerodynamic calculations are performed in OpenVSP and Flightstream. Both programs are used to validate the results. OpenVSP is a software tool used for parametric modeling of aircraft. It is used to design, analyze, and optimize vehicle configurations through 3D modeling and aerodynamic simulation. Flightstream is a computational fluid dynamics (CFD) software specifically designed for aerospace applications, enabling the efficient analysis and optimization of aerodynamic performance. The resulting aerodynamic parameters are calibrated using factors obtained from the reference aircraft ATR-72. Reynolds number and Mach number are calculated using textbook methods [29], [22].

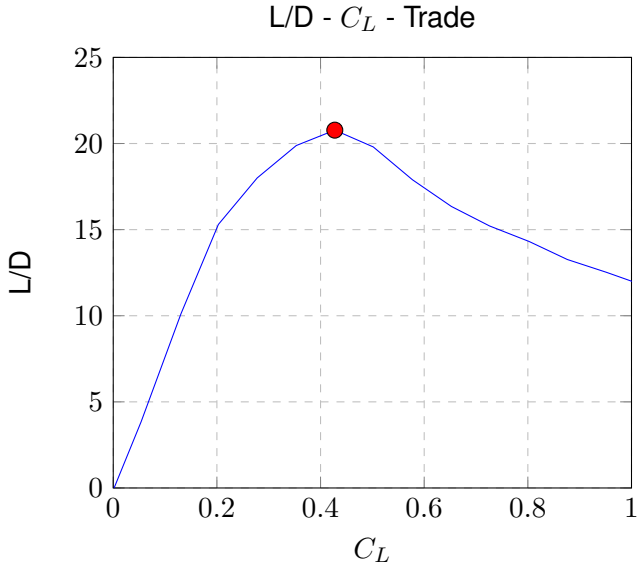

Figure 3.5: L/D - C_L Trade

Figure 3.5 shows that the maximum L/D ratio is approximately $L/D = 20.7$, which occurs at a lift coefficient corresponding to an angle of attack of three degrees. This peak represents the most efficient operating point for the wing. Where the lift generated is high relative to the drag produced. Operating at or near the value corresponding to the maximum L/D ratio is desirable for achieving maximum aerodynamic efficiency. This optimal point can lead to reduced fuel consumption and extended range for aircraft, making it a critical factor in flight planning.
Analysis are performed with aerodynamic data obtained from FlightStream and OpenVSP. Variations between the two softwares are anticipated due to differences in the algorithms and methodologies employed by each software. Additionally, it is crucial to recognize that all computational models are subject to certain degrees of error and approximation. We have decided to prioritize the data generated by FlightStream for our current analysis. This decision is based on the observation that FlightStream's results appear more realistic. To ensure the robustness of our findings, it is essential to conduct further testing and validation with additional simulations and comparisons with wind tunnel test results.

Table 3.3: Breakdown of the total drag

Total drag	
Components	C_D
Center body	0.0027
Outer wing	0.0158
Empennage	0.0008
Fuselage	0.0015
Total	0.0208

Table 3.3 presents a overview of the breakdown of the total drag, specifically detailing conditions observed at an angle of attack of three degrees during the primary flight phase. This demonstrates that the total drag remains relatively low due to the laminar profile, which underlines its effectiveness in minimizing air resistance.

In Table 3.4 below, the mission parameters of the aircraft are presented.

Table 3.4: Performance parameters

Performance parameters		
Parameter	Symbol	Value
Range	R	1500 km
Climb rate @ 4°	ROC	5.0 m/s
Descent rate @ 6°	ROD	7.6 m/s
Cruise speed	v	141.5 m/s (Ma = 0.45)
Cruise altitude	h	6000 m (FL 200)
Lift over Drag	L/D	20.7
Angle of incidence	α_i	2°
Lift coefficient	C_L	0.43
Drag coefficient	C_D	0.0208

Additional Lift

The propeller arrangement on the wing is characterised as so-called distributed propulsion. The advantage of attaching six propeller engines, instead of only two for the ATR-72, is an increased air mass flow over the wing. This generates additional lift.

Table 3.5: Additonal lift by distributed propulsion

Mission stage	Δc_L	$c_{L,tot}$
Takeoff	0.63	0.98
Climb	0.50	0.85
Cruise	0.08	0.43
Descent	0.13	0.64

For the landing approach, the aircraft requires the highest lift coefficient to slow down to the approach speed $v_{landing} = 1.23 v_s = 59 \frac{m}{s}$. The resulting coefficient is $c_{L,Landing} = c_{L,max} = 1.3$.

At that stage the additional lift from the distributed propulsion is not sufficient (Table 3.5). An additional lift of $\Delta c_L = 0.7$ is required. The solution for that are simple moving flaps mounted at the trailing edge of the wing [9]. Due to its simple mechanism there is less complexity and thus less maintenance work caused by the flaps. Still, they generate enough lift and drag for the landing configuration. Additionally the production costs are very low compared to other flap systems because they are in service for long-time and tested in-flight on every aircraft class.

3.4 Propulsion

MOBULA features an innovative and efficient propulsion system. To meet todays requirements of sustainable and eco-friendly air travel the decision was made to a carbon-emission free system of hydrogen and batteries as energy sources. By combining the two propulsion methods valuable synergies are created. The details of the system will be described below.

Operational Considerations

Fuel cell design in modern aircraft applications frequently faces one problem: Since the power output is the main dimensioning factor, the high power demand at takeoff forces the fuel cell to be very large and oversized for cruise flight, where only a fraction of its power is needed. By using batteries for takeoff, climb and descent, MOBULA allows the fuel cell to be tailored precisely to the requirements during cruise. Additionally it is guaranteed, that the fuel cell is primarily used at high altitudes, where the low outside air temperature significantly improves the cooling and therefore its efficiency.
Another problem that aircraft concepts with new propulsion concepts have to deal with is turnaround time. Filling hydrogen tanks and especially charging batteries usually takes a lot of time and makes the aircraft economically unattractive. To avoid long fueling times, MOBULA uses exchangeable tanks and by placing the batteries in the detachable fuselage, the charging time no longer presents an issue. Detailed explanation of the turnaround process can be found in chapter 4.1. In the following sections the detailed design and individual advantages of the propulsion system components are described.

Power Demands

In a first step to dimension the propulsion system the power demands for the mission segments have to be determined. From the design diagram a power loading of 19 $\frac{\mathrm{W}}{\mathrm{N}}$ at the design point can be read. With an estimated maximum takeoff mass (MTOM) of 21.5 t, the maximum power required is 4 MW. This power demand will be needed for takeoff. Since the two PW127 engines of the ATR72 have a combined power output of 3.7 MW [2], this estimation is reasonable. For the required thrust during climb, the following formula can be found:

$$F = mg(\gamma + \frac{1}{E}) \tag{3.1}$$

By using the conversion from thrust to power $F = \frac{P\eta}{v}$ the formula can be written as

$$P = \frac{mgv(\gamma + \frac{1}{E})}{\eta_p} \tag{3.2}$$

With a climb angle $\gamma = 4°$ and a propeller efficiency $\eta_p = 0.8$ the power demand at climb comes to 2.2 MW. The mass in this equation is equal to MTOM, as no mass is lost during the battery powered takeoff. Subsequent calculations will show, that the MTOM value of 21.5 t assumed

for this and further estimations is reasonable.
In cruise flight thrust has to equal drag, which results in the following formula:

$$F = \frac{mg}{E} \tag{3.3}$$

By using the mentioned method to convert the thrust to power, the power demand for cruise flight comes to 1.79 MW. Because of hydrogen consumption, the mass and therefore the required power will decrease during cruise.
During descent phase the power demand is lower. According to [4], the propeller speed at descent is about 40 % lower than at maximum power. This results in a power demand of about $0.216 \cdot P_{max}$ or 0.8 MW. Since electric powered propellers as opposed to turboprop engines – on which this estimation method is based – do not require to stay in idle when no power is needed, the actual power demand of MOBULA may be lower. However, the conservative greater value is used to ensure a sufficiently dimensioned propulsion and energy system. Using the mission parameters v, ROD and ROC from Table 3.4 the times for the segments can be established. The cruise time is based on the average flight duration of the given route network. In the following Figure 3.6 the different mission segments and their power demands are visualized:

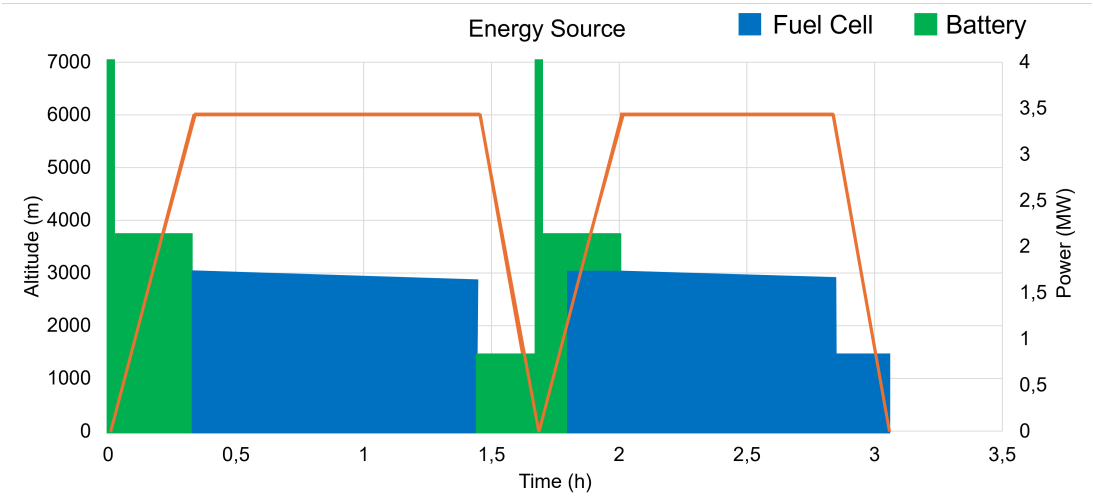

Figure 3.6: Power demand & Energy source used over mission

The breakdown of the total energy consumption is given in Table 3.6. However, the Diversion and Loiter mission is listed here, but is excluded from analysing an average flight. Regarding the 72 seats available it comes down to 41.6 kWh per passenger. Taken into account the average flight distance of 750 km the energy consumption is 5.5 kWh per 100 available seat kilometers (ASK).

Propeller

For the propeller design the ATR-72's engines function as a baseline. The difference is that MOBULA features six instead of two motors. The higher number leads to an increased redundancy in case of single engine failure. It also results in increased additional lift due to the larger swept wing area in the wake of the propellers, as shown in chapter 3.3. That follows the original requirement of implementing distributed propulsion in preliminary design.
Another difference to the ATR design is the blade number. In order to fulfill the TLR of noise reduction (see chapter 2.2) the propeller design is changed. Most important for that is the blade wingtip velocity: $u = 2\Pi\frac{D}{2}N$.

Table 3.6: Energy Consumption over Mission

Energy Consumption	
Section	Consumption [kWh]
Taxi 1	25.0
Takeoff	30.8
Climb	728.8
Cruise	2009.6
Descent	172.7
Taxi 2	25.0
Subtotal	**2992.0**
Takeoff (Diversion)	30.8
Climb (Div)	728.8
Cruise (Div)	1480.1
Descent (Div)	172.7
Total	**5404.5**

Hence, first, the blade number per motor is increased from four to six. Second, the blade diameter is reduced to 2.5 m (ATR- 72-200: 4.0 m) because both values have an essential influence on noise emission.
Another essential criteria is the blade rotation. It depends on propeller static power and the diameter as the main factors. The maximum power output of one engine is 670 kW. Caused by the modified dimensions of the MOBULA propeller motors, the rotation per minute (rpm) is reduced. Compared to the ATR the rotation is now 755 rpm (instead of 1200 rpm), thus a reduction of 37%. Cummulating both effects, the propeller blade tip velocity is decreased by more than 60% compared to the ATR-72 blades. This has a considerable effect on reduced noise emissions [27]. Therefore, fulfilling one of the TLR that were created in preliminary design.
The propellers of the ATR weigh about 164 kg each at a diameter of 4 m. Scaled down, the mass of MOBULA's propellers comes to about 67 kg each or 400 kg in total.

Battery

As Battery technology evolves, we chose the Solid State Battery (SSB) as a promising technology. Compared to Lithium-ion (Li-ion) cells the SSB has a higher energy density with $585\ \frac{\mathrm{Wh}}{\mathrm{kg}}$ predicted for 2040 [15]. Thus, it can store more energy for the electric motors and it is lighter. That makes it a better choice than state-of-the-art Li-ion batteries because using lightweight components is crucial for the total design weight and resulting energy consumption in flight. The SSB also features a higher C-rate (4,0) than other future battery technologies like e.g. the Lithium-Sulfur type. That means that it can be discharged faster, for instance at high power demands at takeoff and climb. Most important it guarantees a higher safety level than Li-ion. That makes it the most suitable choice for our use case [16].

The battery-powered mission segments require a total energy of 1297 kWh, calculated by using the power demand diagram (Figure 3.6). Special attention must be payed on the diversion climb segment, since this is carried out by the fuel cell and the batteries. The energy share is therefore taken into account proportionally. With a system specific energy of $585\ \frac{\mathrm{Wh}}{\mathrm{kg}}$ and a system energy density of $1000\ \frac{\mathrm{Wh}}{\mathrm{L}}$ the battery system has a mass of $2.22\ \mathrm{t}$ and a volume of $1.3\ \mathrm{m}^3$. With an estimated power-to-mass ratio of $2.34\frac{\mathrm{kW}}{\mathrm{kg}}$ the featured battery is capable of producing more than 5 MW of power, which is more than sufficient for this application.

To ensure that the operating temperature stays in a desired range the battery system is placed inside the pressurized fuselage (see Figure 4.3). Since SSB are significantly less flammable than Li-ion batteries, this proposes no further risk to the passengers [31]. Placing the batteries in the fuselage also introduces operational benefits: Primarily it allows the batteries to be charged at the terminal during the boarding process. Also, the batteries can still provide energy for cabin systems like air conditioning when decoupled from the wing part.

Electric Motors

With the rising importance of electric motors in aviation and beyond, research is also increasing. High power and low mass are the key goals. Researchers from MIT have developed an air cooled electric motor capable of delivering 1 MW [10]. With a maximum power demand of 4 MW at takeoff, the motors of MOBULA need an output of 667 kW each. It is therefore a reasonable estimation, that motors in that range will be available by 2050. The developed motor has a power-to-mass ratio of $17\ \frac{\text{kW}}{\text{kg}}$. Applied to MOBULA's electric motors, a total mass of 235 kg or 39 kg each can be estimated.

Fuel Cell System

The Proton Exchange Membrane Fuel Cell (PEMFC) is chosen in this case. Compared to the solid oxide fuel cell it is beneficial in terms of a higher power density and higher TRL [16]. Therefore, the PEMFC is available earlier regarding the EIS. For the dimensions of the fuel cell the power demand in cruise flight is about 1.79 MW. With a gravimetric power density of 2.19 $\frac{\text{kW}}{\text{kg}}$ as mentioned by [15] for the year 2045 the total mass can be estimated as 819 kg. The paper also states a possible volumetric power density of 1.5 $\frac{\text{kW}}{\text{L}}$ by 2045 which results in an approximate total volume of 1,2 m³. Since the propulsion concept of MOBULA features six separate fuel cells installed in a pod behind the propellers, each fuel cell therefore has a mass of 137 kg and a volume of 0.2 m³. The reasons for the podded layout are various. By renouncing a single large fuel cell, valuable space for the hydrogen tanks in the back of the aircraft is created. The placement of the fuel cells behind the propeller also has aerodynamic benefits. Lastly, the change to the outer shape is kept at a minimum, since the fuel cells and the electric motor replace the turboprop engine. The pod-concept is also beneficial for fuel cell cooling. There is an inlet for the incoming air from the front. That air is used to keep the fuel cell in a desired performance range.

Hydrogen Tanks

The sizing of the hydrogen tanks is challenging, as it depends on many variables. Opposed to flying under battery power, in cruise flight the aircraft's mass and therefore its power demand decreases due to the consumption of hydrogen. To account for this we chose to estimate the dimensions of the hydrogen tanks using a modified *Breguet* range equation:

$$R = \frac{\eta_p}{SFC} \cdot E \cdot log(\frac{m_S}{m_E}) \tag{3.4}$$

To estimate the specific fuel consumption (SFC) of hydrogen, [17] takes a detailed systematic approach. An important role here is played by the fuel cell efficiency η_{FC}. This value can vary between 50 % and 60 %, with lower efficiencies for higher power outputs. Since the usage of the fuel cell of MOBULA is limited to the cruise, the power output is relatively constant at the maximum. The efficiency is therefore set to the lower value of 50 %. In the diversion mission, the average efficiency is lowered to 40 % because the fuel cell is additionally operated during

climb and descent which leads to higher outside air temperatures and consequently higher cooling losses. Following the expected developments of parameters like cooling or compressor loss stated in [17] the method returns $SFC_{cruise} = 2.05 \cdot 10^{-7} \frac{\mathrm{N}}{\mathrm{J}}$ and $SFC_{diversion} = 2.56 \cdot 10^{-7} \frac{\mathrm{N}}{\mathrm{J}}$. Using the mentioned breguet equation, we can now calculate mass fractions for the cruise, diversion and loiter segments. For the decrease in cruise the statistical mass fraction for turboprop aircraft during descent was used. Since the specific consumption of hydrogen is about four times lower than the one of fuel-powered turboprop engines, the fraction was modified accordingly. All the mass fractions according to its mission segment are listed in Tab. 3.7.

Table 3.7: Mass fractions for the mission segments

Mission segment	Distance/duration	Mass fraction $\frac{m_{End}}{m_{Start}}$
Cruise	1500 km	0.982
Diversion	250 km	0.996
Loiter	30 min	0.998
Diversion descent	-	0.997
Overall	**-**	**0.973**

The total fuel mass ratio is thus $m_f = 0.027$.
Subsequently the mass of the fuel tanks can be iterated. An MTOM estimation can now be calculated using the maximum zero fuel mass (MZFM) and fuel mass ratio. For the MZFM, the component masses and maximum payload (see Table 3.8) are added together, where an initial arbitrary mass is assigned to the fuel tanks. A contingency of $m_c = 0.05$ is considered.

$$m_{mtom} = \frac{m_{mzfm}}{1 - m_f \cdot (1 + m_c)} \tag{3.5}$$

Due to the low volumetric energy density of gaseous hydrogen, MOBULA – like the majority of current hydrogen aircraft concepts – features a liquid hydrogen tank. The high pressure and low temperatures make the tank design fundamentally different to conventional fuel tanks, as the structure itself constitutes a high fraction of the total mass. This parameter can be quantified as the gravimetric storage density η_{grav} which is defined as the ratio of fuel mass (LH2) to the total system mass (fuel + tank structure). In [17] it is estimated that values up to 0.7 can be reached. For our calculation a gravimetric storage density of 0.5 is used to take a conservative approach and show that the concept is feasible, even if the future development stays below expectations. With η_{grav} and the previously established MTOM, we can calculate the tank mass:

$$m_{tank} = m_{mtom} \cdot m_f \cdot (1 + m_c) \cdot \frac{1}{\eta_{grav} - 1} \tag{3.6}$$

By recalculating alternately MTOM with the updated m_{tank} and vice versa, an iteration process is established, at the end of which an empty hydrogen tank mass of 612 kg is determined. Considering $\eta_{grav} = 0.5$ the maximum capacity is 612 kg of LH2. The iteration process furthermore confirms the for all previous calculations used MTOM of 21.5 t.
The volume of the stored LH2 is about 8,6 m³. To account for insulation and pressure resistance the tank walls have a thickness of 10 cm. The storage is realized by two cylindrical tanks placed in the rear of the wing body. The tank architecture follows the example of the already in-service models in a cylindrical shape because it offers advantages over elliptical forms regarding tank mass and total pressure[32]. The location of the tanks in the rear provides two major advantages: Foremost the tanks can be easily accessed and changed through a flap in the non-pressurized wing part of the airplane. In addition, the safety for the passengers in a crash scenario is increased as they are sitting in front of the tanks.

3.5 Link & Coupling

The airplane is divided into two parts. Serving as the rear part, the wing connects to the back of the fuselage, which acts as the interchangeable part of the connection system. The front part of the plane slides into the back part. A flange ensures a flush closure, minimizing aerodynamic losses. In Figure 3.7 the complete connection process is demonstrated.

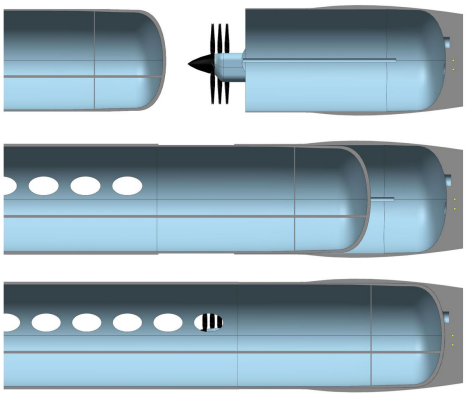

Figure 3.7: Connection process

The connection system consists of three areas: the guide rail, the coupling, and the fixation. The guide rail is placed on the left and right sides of the connection system. It is used to guide the fuselage during connection, putting it in the correct position. Additionally, the fixation mechanism is placed there. The fuselage meets the coupling at the end of the connection system, as shown in Figure 3.7. The coupling is based on the “Scharfenberg Coupling mechanism”, which is usually used for trains. There are three Scharfenberg couplings arranged in a triangular configuration, as shown in Figure 3.8a. Only two of the three couplings are necessary to hold the loads, thereby achieving redundancy. The coupling also functions as an electric connection between fuselage and wing. Therefore, connecting the battery and the cockpit with the propulsion system as well as the control surfaces.

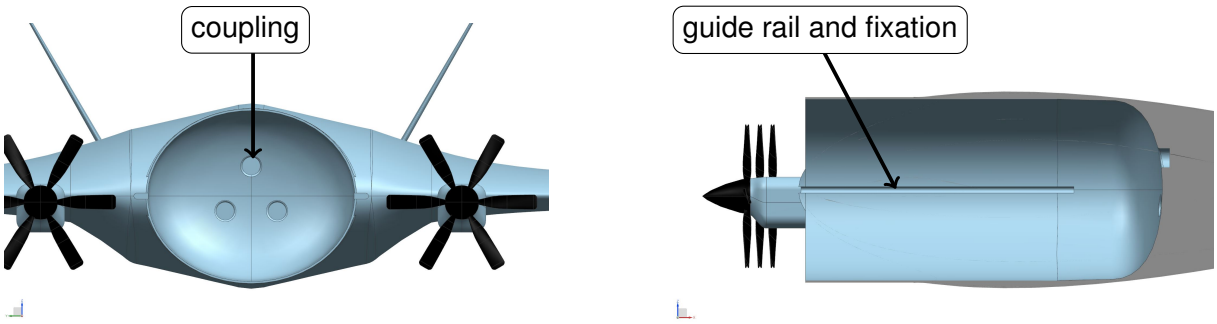

(a) Front view

(b) Side View

Figure 3.8: Connection mechanism on the wing

The loads on a semi-aerobatic plane like this one are $-1.8 < n < 4.5$ [18]. With a maximum takeoff mass of $m_{mtom} = 21500$ kg, this results in a maximum force of $F_{max} = 927.0$ kN. To implement a factor of safety, the load F_{max} is multiplied by a factor of 1.25 to obtain the proof load factor [18]. This means that an actual manufactured structure can withstand the load without any permanent damage. Furthermore, the calculated value is multiplied by a safety factor of 1.5 [18]. This gives us the ultimate load, which in this case is $F_{ultimate} = 1738.2$ kN.

A Scharfenberg coupling mechanism, commonly used in train systems, is designed to handle significant loads, often in the range of hundreds of tonnes. Notably, mechanisms capable of withstanding forces up to 2 MN are already in existence. For instance, the Scharfenberg coupling mechanism used in heavy rail applications is engineered to endure such high forces, as detailed in sources such as [6].

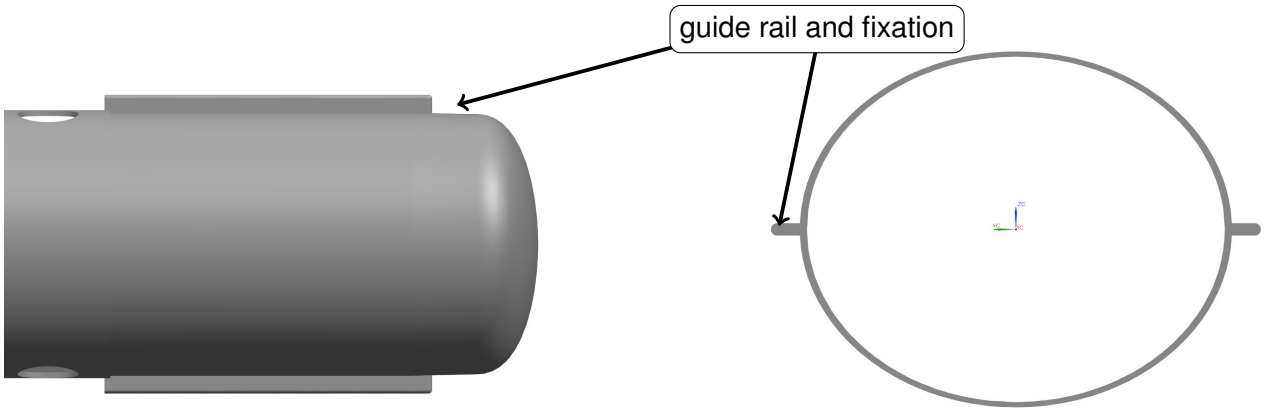

(a) Front view (b) Side View

Figure 3.9: Connection mechanism on the fuselage

Besides being coupled, the front part also has to be fixated in order to have a rigid connection. Therefore, a fixation system is placed alongside the guide rail as illustrated in Figure 3.8b and Figure 3.9. The actual fixation is realized by a hard rubber part that gets pressed from the wing against the guide rail of the fuselage. To release the fixation as well as the coupling, the ground support equipment (GSE) has to be connected. The functionality and design of the GSE are shown in chapter 4.1. With this, another safety mechanism is set in place against an unwanted release. All the described systems together make a quick and safe connection possible.
A *Scharfenberg* coupling system has a typical weight of a around 40 kg [6]. Considering that, the estimates of 200 kg for the airplane's coupling system and 300 kg for the guide rail and fixation system were made conservatively. Therefore, the total weight for the entire connection system, including the coupling, guide rail, and fixation, is estimated at 500 kg.

3.6 Structure

The structural design is divided into two main components: the wing structure and the fuselage structure. Additionally, the connection system presents a challenge, as it must be capable of withstanding all applied loads.
The load-bearing structure of the wing consists of evenly spread ribs across the wingspan. These are connected by beams. To accommodate space for the conduits of the hydrogen tank and the cables for the aileron control, circular cutouts are present in the ribs, as shown in Figure 3.10. In addition, these cutouts contribute to a weight reduction.
The structure to implement the connection system is integrated into the ribs. There is a round structure around the connection parts that takes all the loads and distributes them to the ribs and beams. With this, the connection system is rigidly integrated into the wing structure. Behind the structure of the connection system is a space free of any ribs and beams to provide space for the hydrogen tanks.
For the fuselage, a truss structure design is used. This configuration is selected due to its inherent strength and rigidity, which offers good support and load distribution. At the back part, a special structure is implemented to hold the fuselage part of the coupling system.

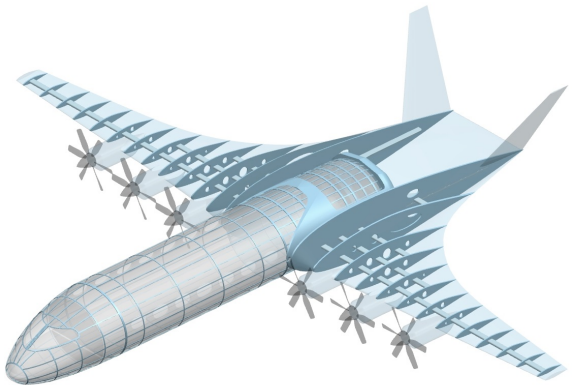

Figure 3.10: Structure

3.7 Mass Breakdown

In the mass estimation, emphasis was placed on the heaviest components. The landing gear was assessed based on data from existing commercial aircraft, where it typically constitutes approximately 2.5% to 5% of the MTOM, as observed in many commercial aircraft [5]. Given the steep descent angle of our aircraft, a more robust and heavier landing gear was selected, accounting for approximately 4% of the MTOM.Details regarding the masses of the propulsion system and hydrogen storage are provided in the chapter 3.4. A breakdown of all component masses and the accumulation to the OME, MZFM and MTOM are given in Table 3.8.

Table 3.8: Aircraft component masses

Component		**Mass [kg]**
Landing gear	Nose landing gear	350
	Rear landing gear	650
Propulsion System	Electric motors	235
	Propellers	400
	Fuel cells	819
	Hydrogen tanks	612
	Batteries	2220
Crew		285
Coupling mechanism		500
Other masses	Structure	8000
	Cabin	
	Cockpit	
	Cables & lines	
OME	**Operating empty mass**	**14071**
Payload	Passengers & luggage	6840
MZFM	**Maximum zero fuel mass**	**20911**
Hydrogen capacity		612
MTOM	**Maximum takeoff mass**	**21523**

The total structural mass was estimated using the structural mass-to-volume ratio of the ATR 72, excluding the engine and landing gear [19]. This ratio was then applied to the volume of the MOBULA airplane. Although the MOBULA has a larger wing volume compared to the ATR 72, which may result in a higher estimated structural mass, this is offset by the increased weight of the structures needed for the hydrogen tank and fuel cell relative to the conventional structures of the ATR 72 [8].

The payload was determined by multiplying the maximum number of passengers by the median expected weight of a passenger and their luggage, resulting in an estimated maximum takeoff mass of approximately 21.500 kg. The payload-range diagram, depicted in Figure 3.11, illustrates the MOBULA Concept aircraft's performance with a design range of 1,500 kilometers. It demonstrates the relationship between payload capacity and achievable range under different loading conditions.

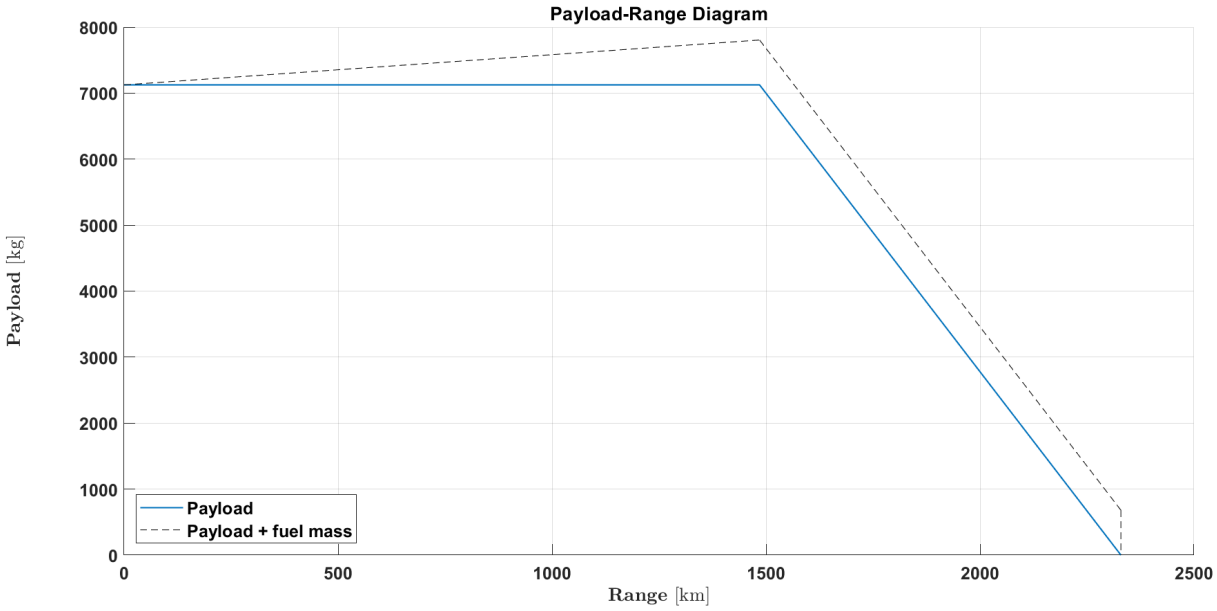

Figure 3.11: Payload-range diagram with design range of 1500 km

4 Operations

From the beginning of the design process smooth operations play a key role in the concept. That is why the design of the aircraft itself and the way of operating it go hand in hand.

4.1 Airport & Boarding Concept

Guided by the top-level requirement for significantly reduced turnaround time, MOBULA adopts an unconventional operational approach. The project features a revolutionary boarding system: the aircraft, divided into a cabin and wing body, utilizes a small vehicle with supportive struts that docks from below at the rear of the cabin upon arrival at the parking position. The vehicle is ground equipment and comparable to a pushback vehicle with additional hydraulic struts surrounding the fuselage (Figure 4.1).

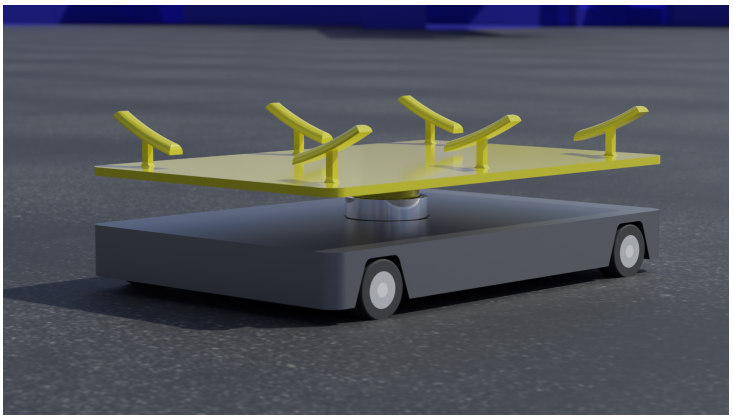

Figure 4.1: Ground Support Equipment

The GSE pushes the cabin out of the wing body and drives it to the airport terminal. The MOBULA concept eliminates the need for passenger bridges, allowing the aircraft to park anywhere, whether in front of the terminal or on the apron. This increases terminal space and enhances airport capacity.
At the lower terminal level, the cabin is moved into the terminal building, allowing passengers to disembark directly. With direct access to the rear cargo area, passengers can retrieve their baggage immediately and exit the airport without delays at the standard baggage claim.

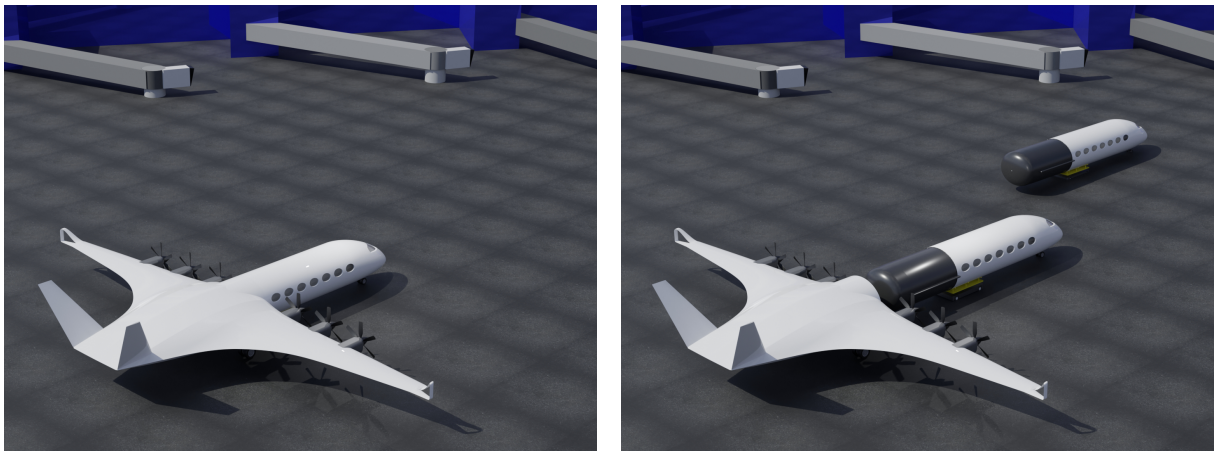

Figure 4.2: Visualization of turnaround operations

While the cabin is already separated from the wing body, the hydrogen tanks are substituted by new ones, which are filled up with LH2 already at the big tank facilities at the airport. As a consequence there is no danger caused by hydrogen refueling at the aircraft itself. There is no risk to passengers during the refueling process as the cabin is not yet attached.
Simultaneously, new passengers board a second cabin body of MOBULA, completing the boarding process a few minutes before departure in the terminal. This in advance boarding streamlines turnaround times and ensures a hassle-free experience for passengers. Additionally, turnaround activities such as catering and sanitary unloading are conducted while the cabin pod is parked in the terminal. By handling these time-consuming procedures prior to boarding, the aircraft's on-ground time is minimized, further optimizing operational efficiency. As soon as the landed MOBULA reaches its parking position, the boarded cabin part stands by nearby, ready to be attached after the refueling process. To streamline operations, two cabin pods are required for each wing body. The docking and detachment process of the cabin pods is illustrated in Figure 4.2.

Adapting to MOBULA requires minimal modifications to airport infrastructure. Specifically, the pushback vehicle must be adapted to handle the cabin part, and modular LH2 tanks must be available for refueling. Notably, no refueling truck needs to approach the aircraft, enhancing safety for passengers and airport personnel. Additionally, the simultaneous execution of many processes significantly reduces turnaround time. The turnaround activities and durations for MOBULA are detailed in Table 4.1.

Table 4.1: Turnaround split

Cumulated turnaround time	
Step	Duration
Docking and detachment	3 min
Refueling & cabin exchange	4 min
Exchange of hydrogen tanks	simultan.
Cabin taxi	simultan.
Coupling cabin to wing body	3 min
Total	**10 min**

As a result, the turnaround time for MOBULA is reduced to 10 minutes, compared to the theoretical 17 minutes for current regional aircraft [25]. This represents a 41% reduction, significantly cutting ground costs for airlines and increasing revenue through more time in the air.

4.2 Cabin Layout

The cabin of MOBULA is embedded in the oval-shaped fuselage in the front part of the aircraft. This distinctive feature is beneficial for placing more seats in a row and shortening the cabin length. The Cross-Section (Figure 4.3b) was designed to fit six seats abreast per row while maintaining a similar seat width and pitch of 43.2 cm and 76.2 cm respectively as featured in the ATR. Using textbook methods from Torenbeek [30], the necessary length of the fuselage, including the flight deck and cabin, was determined to be 18 m. Consequently, it is possible to transport 72 passengers in 12 rows of six seats abreast instead of 18 rows of four seats abreast, while maintaining reasonable seating comfort and aisle width for crew and passenger movement.
Because of MOBULA's unique modular fuselage, the rear part of the cabin doesn't feature any windows, which are important to passenger well-being on board. To compensate for that, the lavatory, galley as well as the baggage compartment are in the rear part of the cabin.

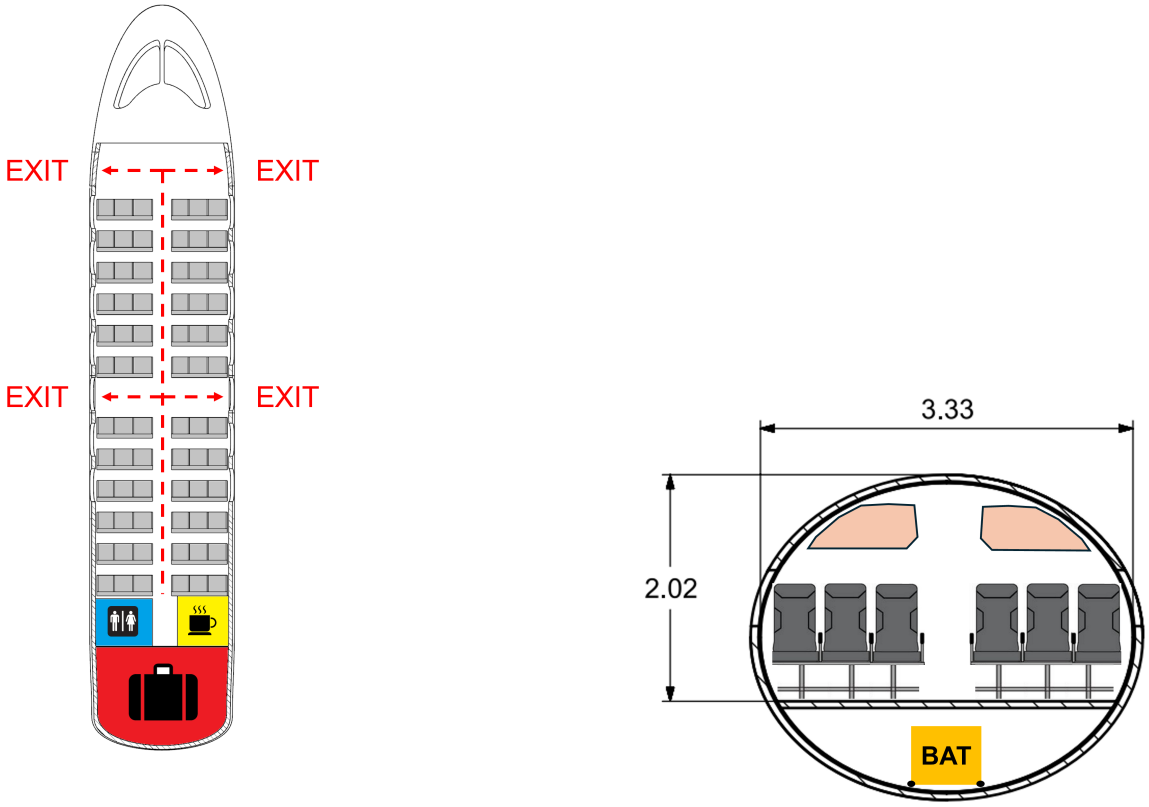

(a) Top View

(b) Front View

Figure 4.3: Cabin Layout

Thus, most of the rows are located next to windows and the rows without direct window access will still get ambient light. According to regulations [CS 25.807] the cabin is equipped with four emergency exits. Two Type I exits are located behind the cockpit and two Type III exits are between rows six and seven, as shown in Figure 4.3a. Each exit does not exceed 1.8 m from the ground, hence no additional assists are necessary for descent to the ground in case of an emergency [CS 25.810].

4.3 Direct Operating Costs

The Direct Operating Costs (DOC) play a crucial role for airlines' operation. Thus it is very important for promising aircraft projects that they are not only ecologically friendly but also economically sound. Conventional cost calculations, as outlined by J. Thorbeck [28], are based on kerosene-powered tube-and-wing aircraft. Given that our concept employs different propulsion technologies, new methods must be applied. A method proposed by Hoelzen et al. [12] incorporates emerging propulsion technologies such as hydrogen and electric energy.
The aircraft can operate throughout the whole year, except for A-, B- and C-Checks that are cumulated in the downtime. There is no night curfew to be considered in this case. This results in a utilization of 136.3 hours per week per aircraft and a total of 3,546 flight cycles annually. A preliminary fleet analysis for the required route network was conducted. The findings indicate that four aircraft are needed to meet market demand, given MOBULA's capacity of 72 seats per flight. The calculated direct operating costs (DOC) associated with these flight cycles are detailed in Table 4.2. The accumulation of DOC result in 2.83 $ per 100 ASK (available seat kilometer).

Table 4.2: Breakdown of Direct Operating Costs

Direct Operating Costs	
DOC_i	Costs [Mio $]
Fuel	0.503
Fees	4.894
Maintenance	1.921
Crew	1.445
Capital	2.089
DOC (1 year)	10.85 Mio
DOC (20 years)	**217.0 Mio**

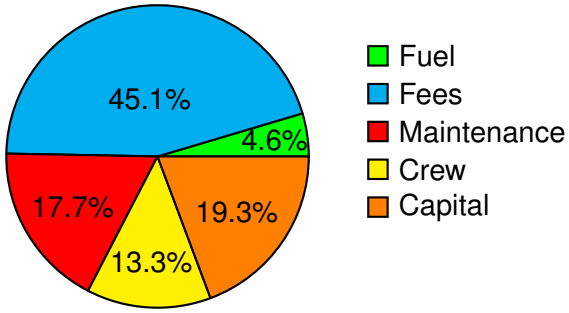

In Table 4.2, maintenance costs are relatively low. This can be attributed to the use of electric powertrains, which generally reduces maintenance requirements compared to gas turbine engines. Electric powertrains have fewer hydraulic lines and lubricated bearings than conventional propulsion systems [24]. Additionally, the development in certification of single pilot operation (SPO) are taken into account calculating the crew costs. With one pilot instead of two pilots flying the aircraft costs for crew are cut significantly. That has direct effect on the total direct operating costs. Moreover, MOBULA's reduced noise emissions around airports are expected to lead to lower landing fees in the future due to anticipated regulatory changes. These potential reductions are not currently included in the operating cost calculations but may be incorporated through revised cost models.

5 Conclusion & Outlook

The initial requirements from preliminary design (Tab. 2.1) are achieved by the MOBULA concept. The completion is shown in Tab. 5.1.

Table 5.1: Fulfillment of requirements

Requirements		
No.	Parameter	Achievement
1	Takeoff distance	✓ (1500 m)
2	Climb angle	✓ (4°)
3	Descent angle	✓ (6°)
4	Average passenger mass	✓
5	Entry into service (2050)	✓
6	Range	✓ (1500km + 250 km Diversion)

MOBULA is a concept of a new way of operating in aviation. In this report, we introduce a new aircraft concept. Unlike traditional designs, this concept features a modular cabin that ensures the aircraft can be adapted to new technologies and environmental standards throughout its operational life. It allows seamless integration with train transportation, including the innovative idea of boarding passengers in the fuselage at the train station and transporting them directly to the aircraft. Challenges for that are naturally in the compatibility of train tracks, but it is not unrealistic to build a safe mechanism for the aircraft structure to drive on tracks.
Overall, the modular concept of the cabin offers a variety of potential applications. While the wing body remains constant the cabin pod is exchangeable. As technologies in structure and materials, but also avionics evolve in the near future, the fuselage can be easily replaced by a modernised cabin version. There is no need of changing the whole aircraft, which saves production costs. The current MOBULA design is based on regional passenger transportation. At the same time, there is the idea of converting the fuselage and therefore the whole aircraft to a freighter variant, which makes it also attractive to cargo companies. Another potential variant is a business and premium model, converting the cabin for business travel. Due to its modularity MOBULA opens up possibilities for multi-functional air operations. The limits are not only set to operate on regional route networks. Looking ahead, the concept can be scaled to larger aircraft and extended to intercontinental flights. This is a lucrative market for airlines due to the rising market demand for intercontinental distances.
For MOBULA it is also considered that single pilot operation (SPO) is certified by 2050. There are already business jets like the "Cessna Citation CJ4" and the "Embraer Phenom 300" that may be flown by only one pilot. As stated in [1] technologies are ready to be implemented in cockpits and regional aircraft are the first to be tested with SPO.
It is essential to note that the low emissions of MOBULA's propulsion system depend on the use of green energy. The power for the battery and to produce green hydrogen has to originate from natural resources. Current developments in renewable energy networks and hydrogen production are convincing to support the green infrastructure needed [21]. The fuel costs were fixed in this task but as shown in [33] they are predicted to decrease and make it more attractive for airline operations. Further, the propulsion of MOBULA is based on a hybrid of battery and fuel cell power. This gives the system the flexibility to respond to future developments in both sectors.

References

[1] Aravind Asokan and Bruce G Cameron. “Single-pilot aircraft in commercial air transport operations: a comparison of Potential Architectures”. In: *Journal of Air Transportation* 31.3 (2023), pp. 113–127.

[2] ATR. *ATR72-Brochure*. URL: https://www.atr-aircraft.com/wp-content/uploads/2020/07/72-210.pdf.

[3] Leopold Böswirth. *Technische Strömungslehre: Lehr- und Übungsbuch ; mit 38 Tabellen*. 7., überarb. und erw. Aufl. Viewegs Fachbücher der Technik. Wiesbaden: Vieweg, 2007. ISBN: 978-3-8348-0272-9.

[4] Willy J.G. Bräunling. *Flugzeugtriebwerke: Grundlagen, Aero-Thermodynamik, ideale und reale Kreisprozesse, Thermische Turbomaschinen, Komponenten, Emissionen und Systeme*. 4. Aufl. 2015. VDI-Buch. Berlin, Heidelberg: Springer Berlin Heidelberg, 2015. ISBN: 9783642345395. URL: http://nbn-resolving.org/urn:nbn:de:bsz:31-epflicht-1495411.

[5] Sonny T. Chai and William H. Mason. “Landing Gear Integration in Aircraft Conceptual Design”. In: MAD 96-09-01 (Sept. 1996).

[6] TU Chemnitz. *Ein Leichtgewicht im Bahnverkehr*. https://www.tu-chemnitz.de/tu/pressestelle/aktuell/4753. Zugriff am: 19. Juli 2024. 2013.

[7] Sam Dakka and Oliver Johnson. “Aerodynamic Design and Exploration of a Blended Wing Body Aircraft at Subsonic Speed”. In: *International Journal of Aviation, Aeronautics, and Aerospace* (2019). DOI: 10.15394/ijaaa.2019.1411. URL: https://commons.erau.edu/cgi/viewcontent.cgi?article=1411&context=ijaaa.

[8] Denis Dilba. “Integrating Hydrogen Propulsion into Aircraft”. In: (Jan. 2021).

[9] Fritz Dubs. *Aerodynamik der reinen Unterschallströmung*. Vol. 1. Springer-Verlag, 2013.

[10] E-Mobility Engineering. *Electric motors for aircraft - E-Mobility Engineering*. 2023. URL: https://www.emobility-engineering.com/electric-motors-aircraft/.

[11] Joel E. Guerrero, Dario Maestro, and Alessandro Bottaro. *Biomimetic spiroid winglets for lift and drag control*. 2012. DOI: 10.1016/j.crme.2011.11.007.

[12] J. Hoelzen et al. “Hydrogen-powered aviation and its reliance on green hydrogen infrastructure – Review and research gaps”. In: *International Journal of Hydrogen Energy* 47.5 (2022), pp. 3108–3130. ISSN: 03603199. DOI: \url{10.1016/j.ijhydene.2021.10.239}.

[13] *Investigation of Boundary-layer Control to Improve the Lift and Drag Characteristics of the NACA 65 (sub 2)-415 Airfoil Section with Double Slotted and Plain ...*. 1950. URL: https://ntrs.nasa.gov/api/citations/19930082766/downloads/19930082766.pdf.

[14] Helmut Kühnelt et al. “Are batteries fit for hybrid-electric regional aircraft?” In: *Journal of Physics: Conference Series*. Vol. 2526. 1. IOP Publishing. 2023, p. 012026.

[15] Valerio Marciello et al. “Design Exploration for Sustainable Regional Hybrid-Electric Aircraft: A Study Based on Technology Forecasts”. In: *Aerospace* 10.2 (2023). ISSN: 2226-4310. DOI: 10.3390/aerospace10020165. URL: https://www.mdpi.com/2226-4310/10/2/165.

[16] Valerio Marciello et al. “Design exploration for sustainable regional hybrid-electric aircraft: A study based on technology forecasts”. In: *Aerospace* 10.2 (2023), p. 165.

[17] Maršenka Marksel and Anita Prapotnik Brdnik. “Maximum Take-Off Mass Estimation of a 19-Seat Fuel Cell Aircraft Consuming Liquid Hydrogen”. In: *Sustainability* 14.14 (2022). ISSN: 2071-1050. URL: https://www.mdpi.com/2071-1050/14/14/8392.

[18] Sudhakar Nair. *Mechanics of Aero-structures*. Cambridge university press, 2015.

[19] Mihaela Florentina Niţă. “Aircraft Design Studies Based on the ATR 72”. In: (June 2008).

[20] Stefano Passerini et al. *Emerging Battery Technologies to Boost the Clean Energy Transition: Cost, Sustainability, and Performance Analysis*. Springer Nature, 2024.

[21] MG Rasul et al. “The future of hydrogen: Challenges on production, storage and applications”. In: *Energy Conversion and Management* 272 (2022), p. 116326.

[22] Daniel P. Raymer. *Aircraft design: A conceptual approach*. Sixth edition. AIAA education series. Reston, VA: American Institute of Aeronautics and Astronautics Inc, 2018. ISBN: 978 1624104909.

[23] G. Redeker et al. *Investigations on high Reynolds number laminar flow airfoils*. 1988. DOI: 10.2514/3.45627.

[24] Ehab Sayed et al. “Review of electric machines in more-/hybrid-/turbo-electric aircraft”. In: *IEEE Transactions on Transportation Electrification* 7.4 (2021), pp. 2976–3005.

[25] Michael Schmidt. “A review of aircraft turnaround operations and simulations”. In: *Progress in Aerospace Sciences* 92 (2017), pp. 25–38.

[26] Michael S. Selig, Mark D. Maughmer, and Dan M. Somers. *Natural-laminar-flow airfoil for general-aviation applications*. 1995. DOI: 10.2514/3.46781.

[27] Vít Štorch et al. “Measurement of noise and its correlation to performance and geometry of small aircraft propellers”. In: *EPJ Web of Conferences*. Vol. 114. EDP Sciences. 2016, p. 02112.

[28] Jan Thorbeck and D Scholz. “DOC-assessment method”. In: *Proceedings of the 3rd Symposium on Collaboration in Aircraft Design, Toulouse, France*. Vol. 19. 2013.

[29] Egbert Torenbeek. *Advanced aircraft design: conceptual design, analysis and optimization of subsonic civil airplanes*. John Wiley & Sons, 2013.

[30] Egbert Torenbeek. *Synthesis of subsonic airplane design: an introduction to the preliminary design of subsonic general aviation and transport aircraft, with emphasis on layout, aerodynamic design, propulsion and performance*. Springer Science & Business Media, 2013.

[31] Johannes Voss. *Solid-state Batteries | Johannes Voss*. 17.07.2024. URL: https://stanford.edu/~vossj/project/solidstate-batteries/.

[32] Christopher Winnefeld et al. “Modelling and designing cryogenic hydrogen tanks for future aircraft applications”. In: *Energies* 11.1 (2018), p. 105.

[33] Moe Thiri Zun and Benjamin Craig McLellan. “Cost projection of global green hydrogen production scenarios”. In: *Hydrogen* 4.4 (2023), pp. 932–960.